

ENG252 Dynamics: Project

Shane Reynolds

October 9, 2019

1 Introduction and Scope

Torsional springs are capable of storing energy if they are displaced by some angle θ beyond their resting position. Letting V_s be the energy stored in a torsional spring, and letting κ be the torsional spring coefficient, Giancoli [1] defines the stored energy in a torsional spring as:

$$V_s = \frac{1}{2} \kappa \theta^2 \quad (1)$$

The scope of this assignment is to use the stored energy in a mousetrap to move a wheeled vehicle 4.5m, deposit a load, and then travel back to the starting point.

2 Design

Mechanical design of the vehicle was informed through online research - a popular approach employed a lever arm attached to the mousetrap. The lever arm applies a moment to the drive shaft via tensioned string, causing the wheels to turn as the mousetrap is de-energised [2]. Complete vehicle construction can be seen in Figure 1. Figures 2 and 3 show a detailed view of the string wound onto the drive shaft; and the mousetrap with attached lever arm, respectively. The main alteration to researched designs saw buffers attached to the drive shaft to increase diameter. This allowed larger drive shaft torque on take off for both initial and return legs of vehicle excursion. Increased torque provides greater angular acceleration, yielding increased linear acceleration assuming no wheel slippage. String is wound around the increased diameter drive shaft just enough so that once vehicle velocity is established the string shifts back to the original shaft size ensuring enough drive shaft rotations to traverse the required distance. The drive shaft set up can be seen in Figure 2.



Figure 1: The vehicle is powered by the torsional spring in the mousetrap. A lever arm is attached to the mousetrap which applies a moment to the drive shaft via the string.

Table 1: Key vehicle characteristics.

Measurement	Value	Unit
Chassis Length	0.45	m
Chassis Width	0.07	m
Chassis Height	0.09	m
Mass	0.185	kg

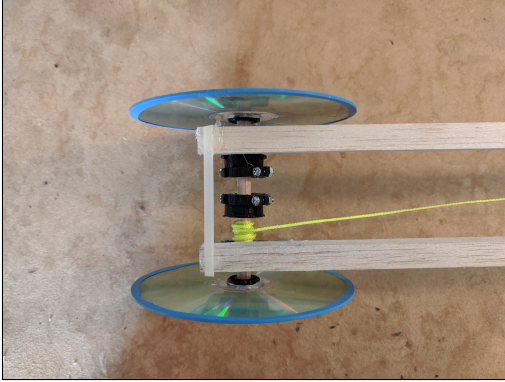


Figure 2: The string is wound around the drive shaft of the vehicle. When the string is tensioned the drive shaft experience torque and subsequent angular acceleration.

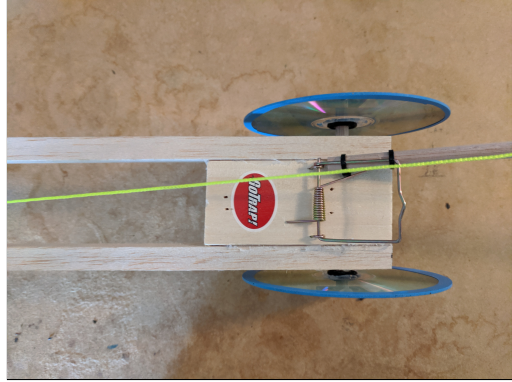


Figure 3: The mouse trap has the dowel lever arm fixed to the side of the mouse trap.

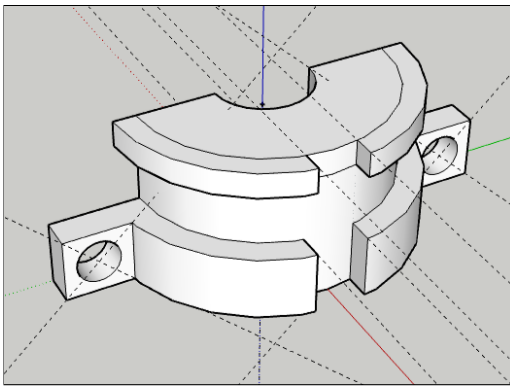


Figure 4: A 3D model of a drive shaft buffer section created using SketchUp.



Figure 5: Wheels were carefully mounted to the shaft ensuring that the wheel centre of mass aligned with the axis of rotation, achieved using 3D printed mounts.

Despite mass increases from the addition of drive shaft diameter buffers, the net result should provide quicker round trip times. Drive shaft buffers were designed to be removed from shaft to allow for easy experimentation. A 3D model of a buffer section, created in SketchUp, can be seen in Figure 4. Compact Discs (CDs) were used as wheels, fit with rubber balloon sections to the outside for increased traction. It was considered important to mount the wheels to shafts through their centre of mass - not doing this would increase the loss of energy to system vibration. Dowel shaft diameters were less than the size of inner CD holes so a custom mount was created ensure axes of rotation were precisely through the CD centre of mass. Figure 5 shows the CD wheels mounted to the shafts, and Figure 6 shows a 3D model of the wheel mounts created in SketchUp.

A further alteration was the inclusion of bearings to reduce rolling friction as the vehicle moves forward. This change reduces the amount of torsional spring energy being lost to work against the rolling friction forces. Information on the bearings can be found in Figure 9. Bearings were mounted to the vehicle chassis using custom designed mounts shown in Figure 7. Additional information on the bearing mounts can be found in Figure 10. Material choices for vehicle design were informed by a rapid prototyping phase in which many different materials were experimented with including aluminium L sections, timber, and balsa wood for the vehicle chassis. Further, both steel, timber, and balsa shafts were trialled. Finally, moving parts, such as pulley systems, created with additive

manufacturing were trialled too. During this rapid prototyping phase it became apparent that performance was greatly influenced by the amount of mass in the vehicle, given the small amount of energy available in the torsional spring. As a result of these findings, a decision was made to strip away all unnecessary moving parts (such as pulleys), and select only the most light weight materials for construction. Balsa was selected for the main chassis, shown in Figure 8. Timber dowels were chosen for the shafts as a compromise between strength and mass, shown in Figure 12. CDs were selected for wheels, as shown in Figure 11. Lightweight custom plastic parts were designed and created using additive manufacturing where possible.

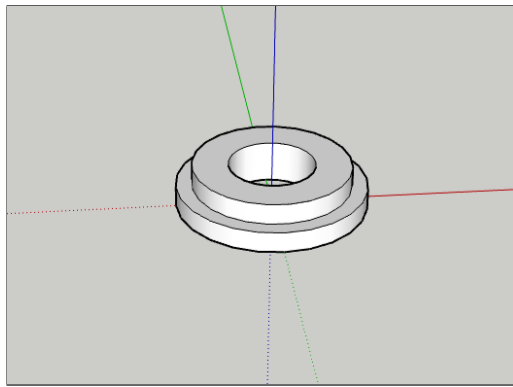


Figure 6: Small plastic mounts designed to securely fix the shaft to the Compact Disc wheel at the centre of mass.

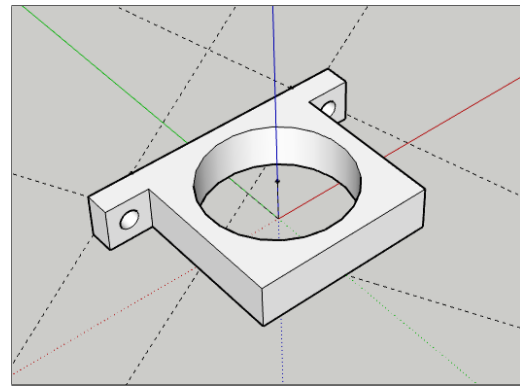


Figure 7: Small plastic mounts designed to house the bearings and attach them securely to the vehicle chassis.

Measurement	Value	Unit
Length	0.450	m
Width	0.010	m
Mass	0.006	kg



Figure 8: Balsa wood section used for the frame. Two lengths were used.

Measurement	Value	Unit
Diameter	0.022	m
Mass	0.009	kg



Figure 9: Bearings used to reduce friction between shafts and frame.

Measurement	Value	Unit
Length	0.028	m
Width	0.028	m
Mass	0.002	kg



Figure 10: Plastic bearing mounts designed with Sketch up and constructed using additive manufacturing. Four of these were used.

Measurement	Value	Unit
Diameter	0.120	m
Mass	0.013	kg



Figure 11: Compact disc used for wheels. Four of these were used.

Measurement	Value	Unit
Diameter	0.008	m
Length (Lever Arm)	0.400	m
Length (Shaft)	0.100	m
Mass (Lever Arm)	0.011	kg
Mass (Lever Arm)	0.003	kg



Figure 12: Dowel lengths used for both the lever arm (one used), and for the shafts (two used) to which wheels were attached.

Measurement	Value	Unit
Length	0.100	m
Width	0.045	m
Mass	0.023	kg



Figure 13: Mouse trap used to power vehicle.

3 Machine Dynamics

3.1 Theoretical Rolling Friction

Rolling friction is the friction experienced by a round body when it rolls across a surface [1]. A rough approximation of the rolling friction coefficient, μ_{rf} , was obtained by placing the vehicle on a flat surface and lifting one end of that surface until the vehicle just starts to move. The experiment set up is shown in Figure 15. Figure 14 shows that if the flat surface length L is known, and the height h is measured just as the vehicle starts to move then β can be determined as:

$$\beta = \arcsin(h/L) \quad (2)$$

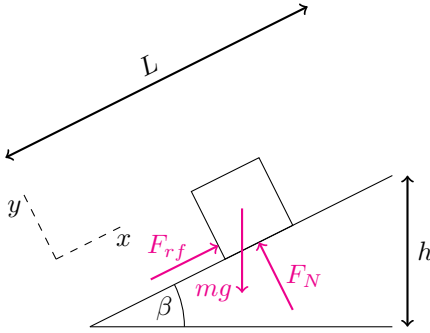


Figure 14: The horizontal surface is raised on an incline until the point at which the vehicle just begins to move. The incline angle and vehicle mass is used to derive an expression for the coefficient of rolling friction.

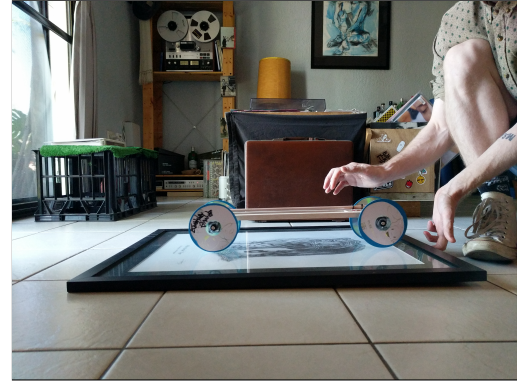


Figure 15: Since bearings were used to reduce rolling friction, the angle of incline is very small as shown here.

Assuming the vehicle does not pass through the inclined surface, we note that:

$$+ \uparrow \sum \mathbf{F}_y = 0 \quad (3)$$

Solving (3) for F_N yields:

$$F_N = mg \cos(\arcsin(h/L)) \quad (4)$$

Similarly, assuming that the vehicle is on the edge of static equilibrium right before it moves allows us to write:

$$\stackrel{\perp}{\rightarrow} \sum \mathbf{F}_x = 0 \quad (5)$$

Noting that $F_{rf} = \mu_{rf} F_N$ we can re-express (5) as:

$$\mu_{rf} F_N = mg \sin(\arcsin(h/L)) \quad (6)$$

Dividing equation (6) by equation (5) yields:

$$\mu_{rf} = \tan(\arcsin(h/L)) \quad (7)$$

Given the length L was measured at 0.75m, and the height h was recorded as 8×10^{-3} m the coefficient of rolling friction was calculated as:

$$\mu_{rf} = 0.011 \quad (8)$$

3.2 Spring Coefficient and Potential Energy

Giancoli defines the moment M created by a torsional spring, for some angle of twist θ from it's equilibrium position, as:

$$M = -\kappa\theta \quad (9)$$

We note that κ is the spring's torsion coefficient, which is also used to determine the potential energy of a torsional spring according to equation (1). To experimentally determine κ for the mousetrap spring, the mousetrap was secured to a bench, and pulley fixed to the trap arm, as shown in Figure 16. Successively greater masses were loaded onto the pulley and the angle θ was measured for each mass. The pulley redirects the force due to gravity, mg , so it is orthogonal along the mousetrap arm. Moments for each mass loading were calculated using equation (9). The experimental data is presented in Table 2.



Figure 16: Experimental setup to determine the mousetrap's torsional spring coefficient.

Table 2: Experimental data captured by loading increasingly larger masses onto the pulley system and measuring the angle of twist from the spring equilibrium position.

Mass [kg]	Force [N]	Moment [N m]	Angle [rad]
0.00	0.00	0.00	0.00
0.09	0.84	0.03	0.15
0.94	0.92	0.04	0.20
0.12	1.22	0.05	0.25
0.22	2.18	0.09	0.52
0.27	2.65	0.11	0.85
0.54	5.32	0.21	1.57
0.61	5.95	0.24	1.89
0.71	7.00	0.28	2.29

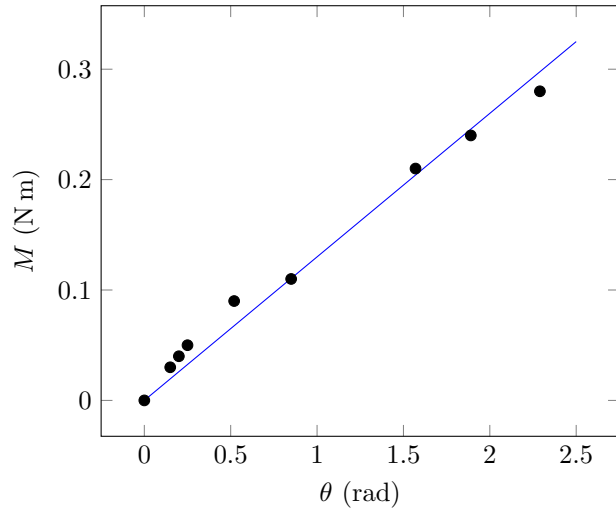


Figure 17: Angular measurements were plotted against calculated moments in order to determine the torsional spring coefficient. Linear regression was employed to fit a straight line model of equation (9) to the data.

Angular measurements were plotted against calculated moments, as shown in Figure 17. Linear regression was used to fit a straight line model, forced through the origin, to the data. We note that this model is experimentally representative of equation (9), for the torsional spring on the mousetrap. The equation was reported as:

$$M = 0.13 \theta \text{ N m} \quad (10)$$

We note that the torsion spring coefficient is $0.13 \text{ N m rad}^{-1}$.

4 Distance Estimation

There are three stages that are considered for vehicle motion. Stage 1 sees the vehicle released from the starting position with a fully energised mousetrap. The string has been wound onto the shaft in a particular direction. The mousetrap de-energises partially, creating kinetic energy, taking the vehicle (and cup) most of the way for the first 4.5m leg of the trip. Stage 2 sees the vehicle's kinetic energy from Stage 1 converted back to potential energy as motion is arrested, and string is wound back onto the shaft. Stages 1 and 2 complete the first 4.5m leg. Finally Stage 3 has the string wound onto the shaft in the opposite direction to Stage 1, and uses the remaining potential energy (plus any energy obtained from Stage 2) to complete the return 4.5m journey. Figure 18 shows Stages 1, 2, and 3 pictorially over the 9m trip, and Figure 19 provides illustration of how the string is wound onto the shaft for Stages 1 and 3.

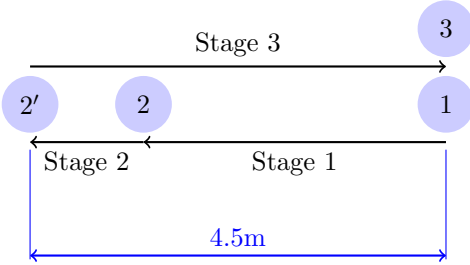


Figure 18: An approximate picture of the ideal situation in which the vehicle travels some distance under the power of the first winding during Stage 1 (from 1 to 2). The kinetic energy takes the vehicle to 4.5m during Stage 2 (from 2 to 2'), where kinetic energy is converted back to elastic potential. Finally, during Stage 3 (from 2' to 3), the remaining potential energy returns the car to the original position.

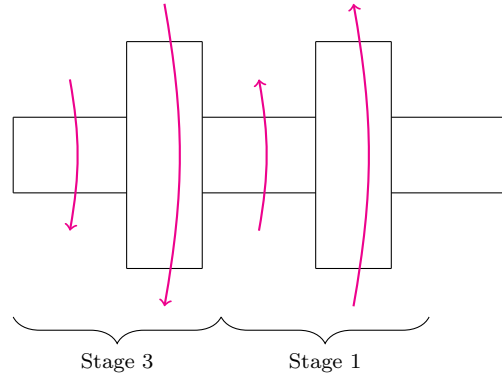


Figure 19: A diagram of the shaft indicating the direction of the string windings onto the shaft. Stage 1 in one direction to make the first 4.5m leg of the trip, and Stage 3 in the opposite direction to make the final leg of the trip.

4.1 Stage 1 (From 1 to 2)

The string will be wound around the drive shaft, as per Figure 19. There will be 3 winds on the large shaft section, and 10 winds on the small shaft section. This means that when the Stage 1 windings are discharged, the vehicle would have travelled a distance, d_1 , evaluated as:

$$d_1 = 13 \times C_{wheel} = 13 \times \pi \cdot 0.12 = 4.9\text{m} \quad (11)$$

This should be just enough to get the entire length of the vehicle (approx 0.4m) over the 4.5m line.

The amount of string unwound, $(d_s)_1$, during Stage 1 is:

$$\begin{aligned}
 (d_s)_1 &= 3 \times C_{big} + 10 \times C_{small} + \epsilon \\
 &= 3 \times \pi D_{big} + 10 \times \pi D_{small} + \epsilon \\
 &= 3 \times \pi \cdot 0.022 + 10 \times \pi \cdot 7.65 \times 10^{-3} + 0.1 \\
 &= 0.55\text{m}
 \end{aligned} \tag{12}$$

Note that ϵ is the result of the string transitioning once from large shaft section to small shaft section, and then back again. The resulting angular displacement of the spring at the end of Stage 1 can be found by considering Figure 20. The thick black line is the lever arm, and the magenta line is the amount of string that has wound off of the drive shaft.

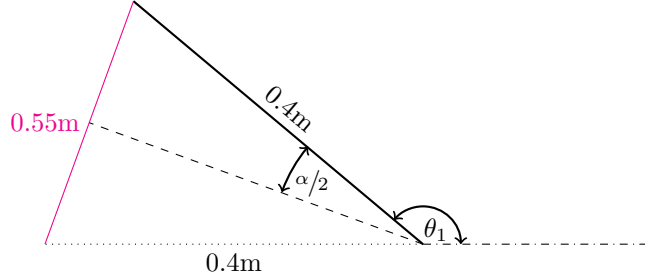


Figure 20: At the end of Stage 1 0.55m of string has been wound off of the drive shaft - this is shown in magenta. Conveniently, the lever arm is the same distance from the centre of the trap to the drive shaft making it easy to calculate θ .

Given that $\theta_1 + \alpha = \pi$, we note that we can determine θ_1 as follows:

$$\theta_1 = \pi - 2 \times \arcsin\left(\frac{0.55/2}{0.4}\right) = 1.63\text{rad} \tag{13}$$

Conservation of mechanical energy allows us to write:

$$(V_s)_1 + T_1 + U'_{1-2} = (V_s)_2 + T_2 \tag{14}$$

We know that the vehicle is initially at rest, and hence $T_1 = 0\text{J}$. The mousetrap spring is energised at an angular displacement of π , and finishes Stage 1 at an angular displacement of 1.63rad . Work is done over the Stage 1 distance as the vehicle is moved against the rolling friction force. Using equation (14) and (1) with values from (8), (10), and (11) we can determine the kinetic energy of the vehicle at the end of Stage 1:

$$T_2 = (V_s)_1 - (V_s)_2 - d_1(\mu_{rf} mg) = 0.37\text{J} \tag{15}$$

4.2 Stage 2 (From 2 to 2')

During Stage 2 kinetic energy at the end of Stage 1 is converted to elastic potential energy by winding up the torsional spring as motion is arrested. We note that:

$$(V_s)_2 + T_2 + U'_{2-2'} = (V_s)_{2'} + T_{2'} \tag{16}$$

At the end of Stage 2 (i.e. 2') the vehicle is at rest implying that $T_{2'} = 0\text{J}$. Assuming the distance from 2 to 2' is small then $U'_{2-2'} \approx 0\text{J}$. Hence, we can determine an approximation for the potential energy for Stage 3 (i.e. the end of Stage 2) as:

$$(V_s)_{2'} = (V_s)_2 + T_2 = \frac{1}{2} \times 0.13 \times 1.63^2 + 0.37 = 0.54\text{J} \tag{17}$$

4.3 Stage 3 (From 2' to 3)

Finally, to find the final distance travelled during Stage 3, we assume all remaining potential energy in the spring will be discharged, and both the initial and final states of the vehicle is at rest, hence $T_{2'} = T_3 = 0\text{J}$. Letting d_3 be the final distance travelled, we note that:

$$(V_s)_{2'} - d_3 \mu_{rf} mg = 0 \quad (18)$$

Rearranging equation (18) allows us to solve for Stage 3 distance:

$$d_3 = \frac{(V_s)_{2'}}{\mu_{rf} mg} = 27.04\text{m} \quad (19)$$

Note the value in (19) would no doubt over estimate the final distance seen in reality. Energy would have been lost to vehicle vibration in Stage 1 and Stage 2. Additionally, the work done in Stage 2 was considered to be 0J - this is not true and some energy would have been lost to rolling friction and not recovered by the torsional spring as assumed. Finally, since the cup was pushed the entire duration of Stage 1 and Stage 2, friction between the cup and the floor would increased coefficient of rolling friction. This last point would most likely have the greatest impact on the potential energy left to spend on Stage 3. Given these considerations, the real value of (19) would therefore be less than 27.04m.

5 Experimental Performance and Possible Improvements

The drive shaft string was wound as indicated in Section 4.1 for Stage 1. The remainder of the string allowed for 2 winds on the large shaft section, and 6 winds on the small shaft section for Stage 3. During execution of Stage 1, vehicle moved as predicted, however, the plastic cup load was buffeted about somewhat. This may have led to increased vehicle vibration and increased friction forces from unanticipated contact of the cup with drive wheels. At the end of Stage 1 the lever arm was at an angle of approximately 1.57rad, which was similar to the predicted value of 1.63rad. Once the cup was delivered a distance of approximately 4.9 m the vehicle velocity was rapidly arrested as the counter winding on the drive shaft converted kinetic energy to potential energy, as per the Stage 2 prediction. The distance travelled during Stage 2 was small. The vehicle was able to easily traverse the final Stage 3 distance of 4.5m, and had considerable kinetic energy remaining when the vehicle was physically stopped. If there was additional space on the track, the vehicle would have most likely traversed another 5m, albeit slowly. Approximately 10m would have been traversed during Stage 3, which is less than the calculated 27.04m, as predicted. A video of the vehicle performance can be seen in the url below:

<https://youtu.be/c6lqrsZ5jxA>

The vehicle was released at 0.07 s into the video and completes the trip at 0.22 s into the video, resulting in a 15 s round trip time. Summarised values of the trial can be found in Table 3. After observing the vehicle in action it is apparent that reducing rolling friction by creating a lightweight mechanism to support the cup during Stages 1 and 2 would significantly improve vehicle performance. Additionally, further reduction of vehicle mass would also help. Other improvements that could have a minor improvement on performance include ensuring that the wheels are orthogonal with the ground to limit vibration when in motion; and more precise construction techniques to reduce rolling friction due to shaft misalignment.

Table 3: Recorded trip time to cover Stages 1, 2, and 3

Description	Value	Unit
Stage 1 Distance	4.9	(actual) m
Stage 3 Distance	10.0	(estimated) m
Round trip time	15.0	(actual) s

6 Conclusion

The potential energy stored in an energised mousetrap is more than enough to transport a small plastic load 4.5m using a vehicle, and then return the vehicle to it's starting position. The two most important considerations when designing a vehicle suitable for this task is to reduce mass, and reduce friction. To reduce overall trip time it is important to use a larger sized shafts to increase angular acceleration on take off, and then switch back to a smaller sized shaft once the vehicle is at sufficient velocity. This comes at the addition of some mass, and the loss of some energy during gear changes. Finally, to achieve accurate predictions traversed distances more experimental data regarding operating conditions should be collected to ensure that all energy events are factored into the modelling. Simplifying assumptions can lead to over estimations.

References

- [1] D. C. Giancoli, “Physics for scientists and engineers 3rd edn.,” *Prentice Hall*, 2000.
- [2] “Doc fizzix: Mousetrap car,” <https://www.docfizzix.com/>.